

Alma Mater Studiorum Università di Bologna  
Archivio istituzionale della ricerca

Expression of CLAVATA3 fusions indicates rapid intracellular processing and a role of ERAD

This is the final peer-reviewed author's accepted manuscript (postprint) of the following publication:

*Published Version:*

Francesca De Marchis, S.C. (2018). Expression of CLAVATA3 fusions indicates rapid intracellular processing and a role of ERAD. PLANT SCIENCE, 271, 67-80 [10.1016/j.plantsci.2018.03.020].

*Availability:*

This version is available at: <https://hdl.handle.net/11585/632495> since: 2019-06-03

*Published:*

DOI: <http://doi.org/10.1016/j.plantsci.2018.03.020>

*Terms of use:*

Some rights reserved. The terms and conditions for the reuse of this version of the manuscript are specified in the publishing policy. For all terms of use and more information see the publisher's website.

This item was downloaded from IRIS Università di Bologna (<https://cris.unibo.it/>).  
When citing, please refer to the published version.

(Article begins on next page)

This is the final peer-reviewed accepted manuscript of:

De Marchis F., Colanero S., Klein E.M., Mainieri D., Prota V.M., Bellucci M., Pagliuca G., Zironi E., Gazzotti T., Vitale A., Pompa A., 2018. Expression of CLAVATA3 fusions indicates rapid intracellular processing and a role of ERAD. *Plant Science* 271, 67–80. DOI: 10.1016/j.plantsci.2018.03.020

The final published version is available online at:

<https://doi.org/10.1016/j.plantsci.2018.03.020>

© 2018. This manuscript version is made available under the Creative Commons Attribution-NonCommercial-NoDerivs (CC BY-NC-ND) 4.0 International License (<http://creativecommons.org/licenses/by-nc-nd/4.0/>)

# Expression of CLAVATA3 fusions indicates rapid intracellular processing and a role of ERAD

Running title: CLAVATA3 processing

Francesca De Marchis<sup>a</sup>, Sara Colanero<sup>a</sup>, Eva M. Klein<sup>b</sup>, Davide Mainieri<sup>b</sup>, Viviana M. Prota<sup>b</sup>, Michele Bellucci<sup>a</sup>, Giampiero Pagliuca<sup>c</sup>, Elisa Zironi<sup>c</sup>, Teresa Gazzotti<sup>c</sup>, Alessandro Vitale<sup>b,\*</sup> and Andrea Pompa<sup>b,\*</sup>

<sup>a</sup>Istituto di Bioscienze e Biorisorse, Consiglio Nazionale delle Ricerche, Perugia, Italy

<sup>b</sup>Istituto di Biologia e Biotechnologia Agraria, Consiglio Nazionale delle Ricerche, Milano, Italy

<sup>c</sup>Dipartimento di Scienze Mediche Veterinarie, Università di Bologna 40064 Ozzano Emilia (BO) Italy

\*Corresponding authors.

*E-mail address:* [andrea.pompa@ibbr.cnr.it](mailto:andrea.pompa@ibbr.cnr.it) (A. Pompa) [vitale@ibba.cnr.it](mailto:vitale@ibba.cnr.it) (A. Vitale)

## Highlights:

- Tobacco expressing CLAVATA3-GFP (CLV3-GFP) secretes the active CLV3 peptide
- The ER chaperone endoplasmic reticulum supports CLV3-GFP synthesis
- Intact CLV3-GFP is rapidly degraded, also when intracellular traffic is inhibited
- CLV3-GFP half-life is extended by inhibitors of ER associated degradation (ERAD)
- We propose that ERAD regulates the synthesis of the active CLV3 peptide

## ABSTRACT

The 12 amino acid peptide derived from the *Arabidopsis* soluble secretory protein CLAVATA3 (CLV3) acts at the cell surface in a signalling system that regulates the size of apical meristems. The subcellular pathway involved in releasing the peptide from its precursor is unknown. We show that a CLV3-GFP fusion expressed in transfected tobacco protoplasts or transgenic tobacco plants has very short intracellular half-life that cannot be extended by the secretory traffic inhibitors brefeldin A and wortmannin. The fusion is biologically active, since the incubation medium of protoplasts from CLV3-GFP-expressing tobacco contains the CLV3 peptide and inhibits root growth. The rapid disappearance of intact CLV3-GFP requires the signal peptide and is inhibited by the proteasome inhibitor MG132 or coexpression with a mutated CDC48 that inhibits endoplasmic reticulum-associated protein degradation (ERAD). The synthesis of CLV3-GFP is specifically supported by the endoplasmic reticulum chaperone endoplasmin in an *in vivo* assay. Our results indicate that processing of CLV3 starts intracellularly in an early compartment of the secretory pathway and that ERAD could play a regulatory or direct role in the active peptide synthesis.

**Abbreviations:** BFA, Brefeldin A; CLV3, *clavata3*; ER, endoplasmic reticulum; ERAD, endoplasmic reticulum associated degradation; GFP, green fluorescent protein;

**KEY WORDS:** *Arabidopsis thaliana*; CLAVATA3; endoplasmin; ERAD; protein processing; protein traffic

## 1. Introduction

The soluble secretory protein CLAVATA3 (CLV3) cooperates with a number of plasma membrane proteins in a signalling mechanism that limits excessive proliferation of pluripotent cells in apical meristems [1]. CLV3 was the first discovered member of the large CLE protein family (CLE being the acronym for CLAVATA3/ENDOSPERM SURROUNDING REGION-related), short soluble proteins with a signal peptide for entry into the secretory

pathway [2,3]. A 12-14 amino acid peptide located in the C-terminal region is released post-translationally from CLE proteins and is responsible for their biological activities. The active 12 amino acid peptide of CLV3 [4] is recognized extracellularly by the ectodomains of the plasma membrane receptor kinases CLV1 and BAM1, in a process that also involves the co-receptors CLV2, CORYNE and RPK2 [4-6]. The pathway and subcellular localization of CLV3 processing is however not easy to define [7-10], also because antibodies for the CLV3 or other CLE polypeptides are not available. CLE19 C-terminal processing involves the SOL1 protease, which is located in endosomes [11]. However, sol1 mutations suppress the phenotype generated by CLE19 overexpression but not that of CLV3 overexpression, indicating that SOL1 is necessary for maturation of the former but not the latter [11]. CLV3 expressed in *E. coli* without its signal peptide and with added N-terminal Trx and His tags was processed giving rise to the active peptide when added to the growth medium of Arabidopsis seedlings [12]. Therefore, the precursor can be correctly processed extracellularly by secreted proteases. Other tagged versions of CLV3 or its C-terminal region expressed in *E. coli* were used to determine *in vitro* the activity of plant extracts or incubation media of plant cell cultures [9,10]. The results indicate that a secreted serine protease is able to perform N-terminal processing, while C-terminal processing may involve a progressive carboxypeptidase of yet unknown localization [10].

To determine whether, after insertion into the endoplasmic reticulum (ER) and removal of the signal peptide, CLV3 undergoes further processing before reaching the extracellular space, we have analysed the *in vivo* destiny of CLV3-GFP fusions expressed in transgenic tobacco or transiently in plant protoplasts.

## **2. Materials and methods**

### ***2. 1. Tobacco transformation***

Plasmid pAVA120, in which the cDNA coding for CLV3 had been inserted ahead of the GFP sequence [7] was used to excise by *Pst*I a fragment

including the 35S promoter, the sequence encoding CLV3-GFP and the 35S terminator. This fragment was introduced into the *Pst*I site of the pGreenII binary vector [13], obtaining pGreen.CLV3-GFP. *Agrobacterium tumefaciens* strain GV3101 transformed with pGreen.CLV3-GFP, was used to produce transgenic *Nicotiana tabacum* cvSR1, as described [14].

## 2. 2. Transient expression in protoplasts and pulse-chase labelling

Plasmid pAVA120 encoding CLV3-GFP or CLV3 $\Delta$ sp-GFP [7] and plasmid pDHA encoding mGFP5 [15] or T343F phaseolin [16] have been described. To produce CLV3-mGFP5, the 408 bp region between the *Nde*I/*Bsa*I sites of pGreen.CLV3-GFP was substituted with the similarly restricted fragment from pDHA.mGFP5 [15]. CLV3-mGFP5 thus contains the three stabilizing mutations of mGFP5 [17]. The coding sequence of CLV3-FLAG, consisting of the CLV3 precursor immediately followed by the FLAG epitope (DYKDDDDK) before a stop codon, was synthesized (Integrated DNA Technologies) and inserted into *Sa*II/*Sph*I-restricted pDHA.

Transient expression was performed in protoplasts prepared from 4-7 cm-long leaves of wt tobacco plants cultivated in axenic condition or protoplasts similarly isolated from transgenic plants, using polyethylene glycol-mediated transfection as described [18]. Transfected protoplasts (usually 1 million l<sup>-1</sup>) were incubated overnight in K3 medium (Gamborg's B5 basal medium with minimal organics [Sigma], supplemented with 750 mg l<sup>-1</sup> CaCl<sub>2</sub>·2H<sub>2</sub>O, 250 mg l<sup>-1</sup> NH<sub>4</sub>NO<sub>3</sub>, 136.2 g l<sup>-1</sup> sucrose, 250 mg l<sup>-1</sup> xylose, 1 mg l<sup>-1</sup> 6-benzylaminopurine, and 1 mg l<sup>-1</sup> 1-naphthalenacetic acid, pH 5.5), before pulse-labelling for 1 h with [<sup>35</sup>S]Met and [<sup>35</sup>S]Cys (Pro-Mix; Amersham Biosciences, final concentration of 100  $\mu$ Ci mL<sup>-1</sup>) at 25°C, in K3 medium supplemented with 150  $\mu$ g ml<sup>-1</sup> bovine serum albumin. Chase was performed by adding unlabelled Met and Cys to final concentrations of 10 mM and 5 mM respectively. At each chase point, three volumes of ice-cold W5 medium (154 mM NaCl, 5 mM KCl, 125 mM CaCl<sub>2</sub>·2H<sub>2</sub>O, and 5 mM glucose) were added and centrifugation performed at 60 g for 10 min. Precipitated protoplasts and their supernatant, which contains proteins

secreted during pulse-chase, were collected and homogenized at 4°C by adding 2 volumes of ice-cold protoplast homogenization buffer [16] supplemented with Complete protease inhibitor cocktail (Roche). Treatments of protoplasts with BFA (Roche, 10 µg ml<sup>-1</sup> final, stock solution 2 mg ml<sup>-1</sup> in ethanol), wortmannin (Sigma-Aldrich, 10 µM final, stock solution 1 mM in dimethyl sulfoxide) or MG132 (Sigma-Aldrich, 100 µM, stock solution 10 mM in dimethyl sulfoxide) were performed by adding the inhibitors 45 min before pulse-labelling, and maintaining the same concentrations throughout the chase. For the CDC48 assay, protoplasts were transiently transfected with 30 µg plasmid encoding CDC48wt or CDC48QQ [19], incubated overnight in K3 at 25°C and pulse-labelled for 1 h. Immunoselection was with rabbit anti-GFP serum (Life Technologies), rabbit anti-FLAG polyclonal antibodies (Sigma–Aldrich), or rabbit anti-phaseolin serum [16], followed by incubation with Protein A Sepharose (Invitrogen). Solubilization of insoluble material by SDS and reducing agent followed by immunoselection was performed as described [20]. Immunoselected proteins were separated by 15% acrylamide SDS-PAGE in reducing conditions, using <sup>14</sup>C-methylated proteins (Sigma-Aldrich) as molecular mass markers. Radioactive proteins were detected and quantified either using the Starion FLA-9000 phosphoimager system and Multi Gauge Ver.2.0 (Fujifilm), or by treatment with 2,5-diphenyloxazole and fluorography as described [16] and quantitation using TotalLab Quant (TotalLab, Newcastle upon Tyne, UK) or ImageJ open source software (imagej.net).

### 2.3. Chaperone assay

Each plasmid mixture was composed of 20 µg of plasmid encoding CLV3-GFP or mGFP5, 20 µg encoding Arabidopsis endoplasmic reticulum BiP (pDE800; [21]), and the needed amount of plasmid encoding α-amylase (pNL200; [21]) as a secretory protein with no chaperone activity, to reach final 60 µg and thus maintain a roughly constant amount of total recombinant protein translocated into the ER lumen. After transfection and 4 h recovery, protoplasts were incubated for 16 h in K3 medium in the

presence of 20  $\mu\text{g mL}^{-1}$  tunicamycin (Sigma, from a 5 mg  $\text{mL}^{-1}$  stock dissolved in 10 mM NaOH) or an equivalent volume of 10 mM NaOH. Protoplasts were then pulse-labelled for 1 hr at 25°C with the [ $^{35}\text{S}$ ]Met and [ $^{35}\text{S}$ ]Cys mixture, homogenized as described above and subjected to immunoselection using anti-GFP, anti-BiP [16] or anti-endoplasmic reticulum [18]. After SDS-PAGE and fluorography, intensities of bands were measured using TotalLab Quant software.

#### *2.4. Protein blot*

When needed, BFA or wortmannin was added to the protoplast incubation medium 1 h after transfection at the concentrations described above and maintained at the same concentration throughout the incubation. Protoplast homogenization was performed as described above. To analyze proteins from plants, total proteins were extracted from plant tissues by homogenization in ice-cold plant homogenization buffer (200 mM NaCl, 1 mM EDTA, 0.2% Triton X-100, 2% 2-mercaptoethanol, 100 mM Tris-Cl pH 7.8, supplemented with Complete protease inhibitor cocktail), using a buffer/fresh tissue ratio of 4 ml/g. After centrifugation at 1,500 g, 4°C for 10 min, the resulting supernatant was considered as the total protein extract. For protein blot, proteins were separated by SDS-PAGE and then electrotransferred into nitrocellulose membrane (PerkinElmer). Protein Molecular Weight Markers (Fermentas) were used as molecular mass markers. Proteins were detected using rabbit anti-GFP polyclonal serum (A6455, 1:2,000 dilution, Molecular Probes) or rabbit anti-phaseolin polyclonal serum raised against phaseolin purified from bean cotyledons ([16], 1:5,000 dilution) and Super West Pico chemiluminescence substrate (Pierce). Chemiluminescence was detected using the ChemiDoc XRS+ Imaging System (BioRad).

#### *2.5. Fluorescence microscopy*

Confocal laser scanning microscopy of shoot apex of transgenic tobacco expressing CLV3-GFP was performed using a Nikon Eclipse Ti2



microscope, equipped with a Nikon A1+ laser scanning device (Nikon, <http://www.nikon.com/products/microscope-solutions/lineup/confocal/a1/index.htm>). GFP and chlorophyll were excited with the 488 nm laser and the emission was collected at 505-535 nm and 620-700 nm, respectively using the GaAsP A1-DUVB-2 tunable emission detector. The pinhole was set to 1.2 airy unit. Images were acquired by a CFI PLAN APO 20X VC dry objective and were analyzed using Fiji software (<https://fiji.sc/>). For fluorescence microscopy, transfected tobacco protoplasts were incubated for 24 h in K3 medium, concentrated by the addition of three volumes W5 medium followed by centrifugation at 60 g for 10 min, and then observed by epifluorescence microscopy using a Zeiss Axiovert 200M microscope (Carl Zeiss) equipped for epifluorescence and AxioVision 40 software (version 4.8.2.0, Carl Zeiss Microimaging).

## *2.6. Immunocytochemistry*

Protoplasts isolated from CLV3-GFP transgenic tobacco were incubated overnight in K3 before adding MG132 to 100  $\mu$ M final concentration, or an equivalent volume of dimethyl sulfoxide as a control. After 2 h incubation, immunocytochemistry was performed as described [22] except that the anti-GFP primary antibody was added at 1:1,000 dilution. Cells were visualized with a Zeiss PALM Microbeam Axio-observer.Z1 fluorescence microscope equipped with a 633 oil-immersion objective. Images were collected with an AxioCam MRm 60N-C 1"1, ox camera (Zeiss) and visualized with AxioVision software.

## *2.7. Subcellular fractionation*

Subcellular fractionation was performed by isopycnic gradient ultracentrifugation. Young leaves of transgenic tobacco expressing CLV3-GFP were homogenized with buffer without detergent (12% sucrose, 10 mM KCl, 2 mM MgCl<sub>2</sub>, 100 mM tris-Cl, pH 7.8). About 1 ml of homogenate was loaded in the top of a 16-55% (w/w) continuous sucrose gradient. After ultracentrifugation at 141,000g for 4 h at 4°C, fractions of 780  $\mu$ l were

collected. An equal aliquot of each fraction was separated by SDS- PAGE and then analyzed by protein blot with anti-GFP antiserum.

### 2.8. Root growth assay

Seeds of *Arabidopsis thaliana* (Col-0) were sterilized as described [23] and imbibed in sterile distilled water at 4°C in dark for 2 days before plating on half-strength MS basal salts medium (Sigma-Aldrich, USA), pH 5.8, plus 1% sucrose, 0.5 g l<sup>-1</sup> MES (Merck, Germany) and 1.5% agar. Three million protoplasts isolated from transgenic CLV3-GFP or wt tobacco plants were incubated for 3 days at 25°C in the dark. These protoplast incubation media or 50 nM CLV3P synthetic peptide were added to the MS substrate before pouring it. Seedlings were grown in a vertical position at 25 °C and 16-h light /8-h dark photoperiod for 10 days before root length measurement.

### 2.9. LC MS/MS analysis

Incubation medium of about 6 million protoplasts isolated from CLV3-GFP transgenic or wt protoplasts incubated for 3 days at 25°C in the dark, was precipitated with an equal volume of TCA (100%). After two washes with cold acetone the pellets were resuspended in 100 µl of double-distilled water, samples were diluted 1:10 with a solution acetonitrile:water (60:40) with 0.1% formic acid. Ten µl of sample were analysed using an Acquity Ultra-performance liquid chromatographer coupled with Quattro Premiere XE, a triple quadrupole, using a Waters BEH C18 column (1.7 µm, 2.1 x 50 mm) equipped with a guard column of the same type (Waters Corporation, Milford, USA). The separation was carried out in programmed condition with a flow rate of 0.2 ml min<sup>-1</sup> and mobile phase consisting of water/formic acid 0.1% (A) and acetonitrile/formic acid 0.1% (B). The gradient was T0 min: 97% A, 3% B, T1 min: 97% A, 3% B, T4 min: 30% A, 70% B, T5 min: 97% A, 3% B. All analyses were conducted in positive electrospray ionization mode (ESI+) using selected reaction monitoring (SRM). The optimized mass spectrometer conditions for CLV3 were: Transition (m/z) 656,8 > 503,0, Cone Voltage 32 V, Collision Energy 24 eV; capillary voltage 2.5 kV. Nitrogen was used as

desolvation gas ( $350 \text{ l h}^{-1}$ ) and cone gas ( $150 \text{ l h}^{-1}$ ) while the collision gas was argon (flow rate of  $0.35 \text{ ml min}^{-1}$ ). Data acquisition processing was performed using Mass Lynx 4.1 Software.

### 3. Results

#### 3.1. *CLV3-GFP undergoes rapid proteolysis in vivo*

CLV3-GFP [7] is composed of CLV3 fused to the N-terminus of mGFP4. A similar construct under the control of the endogenous CLV3 promoter is able to rescue *clv3* mutant Arabidopsis plants [8], indicating that fusion to GFP does not affect the production of the active peptide and can therefore be used to investigate the time-course of GFP processing. The deleterious effects of CLV3 overexpression in Arabidopsis make biochemical and cell biology analysis very difficult. We therefore transiently expressed CLV3-GFP in tobacco protoplasts. We first determined whether CLV3-GFP could be detected by immunoprecipitation. GFP with a transient N-terminal signal peptide for translocation into the ER was also expressed, as a control secretory form of GFP (mGFP5, [15]). Transfected protoplasts were incubated for 1 h with a mixture of [ $^{35}\text{S}$ ]Met and [ $^{35}\text{S}$ ]Cys and proteins were immunoselected with anti-GFP serum from a total cell homogenate (Fig. 1A). Major polypeptides with the predicted molecular mass were immunoselected: 35 kD (filled arrowhead, CLV3-GFP) and 28 kD (empty arrowhead, mGFP5).

To elucidate the destiny of CLV3-GFP, protoplasts were subjected to 1 h pulse followed by different chase time-points. Intact CLV3-GFP rapidly disappeared during the chase, with no signs of its secretion or intracellular accumulation of immunoprecipitable fragments (Fig. 1B). mGFP5 is an improved GFP, with three point mutations to avoid misfolding and precipitation at temperatures above  $30^\circ\text{C}$  [17]. mGFP4, which is the GFP version present in CLV3-GFP, is instead the unmodified version. Although constructs containing mGFP4 are widely used in plant biology (for CLV3 see

[7, 8]) and the experiments presented here are conducted at 25°C, we produced two new CLV3 fusions. CLV3-mGFP5, contains the three stabilizing point mutations of mGFP5, whereas CLV3-FLAG was constructed by adding at the end of the CLV3 precursor the DYKDDDDK FLAG epitope, followed by a stop codon. In protoplasts, CLV3-mGFP5 rapidly disappeared during the chase, without any detectable secretion both in tobacco (Fig. 1C) and Arabidopsis (Fig. S1) protoplasts. CLV3-FLAG was also not secreted, even if it was intracellularly slightly more stable than the GFP fusions (Fig. 1D). About 50% of newly synthesized CLV3-FLAG were lost in the first 2h of chase, compared to 80% in the case of CLV3-GFP (Fig. 1E). Therefore, the appended sequence has some influence on the rate of disappearance, but the lack of secretion of intact polypeptides is a common characteristic of the three fusions tested and none of them seems to have high intracellular stability. Subsequent experiments were performed using CLV3-GFP.

As expected and shown previously [15], newly synthesized mGFP5 is gradually secreted by protoplasts during the chase (Fig. 2A). To determine whether the synthesis of CLV3-GFP has an unexpected negative effect on the secretory pathway, we therefore co-expressed mGFP5 and CLV3-GFP. The CLV3 fusion does not inhibit mGFP5 secretion (Fig. 2B). To verify whether translocation into the ER is necessary for CLV3-GFP degradation, a construct in which the CLV3 signal peptide has been deleted (CLV3 $\Delta$ sp-GFP, [7]) was expressed. CLV3 $\Delta$ sp-GFP was much more stable than CLV3-GFP (Fig. 2C, and compare with panel 2B), indicating that the disappearance of CLV3-GFP requires a transient signal peptide for insertion into the ER.

To confirm the pulse-chase results, transfected protoplasts were analysed by protein blot, which measures steady state protein levels, and by fluorescence microscopy, which detects active GFP. Protein blot indicated that a much higher amount of CLV3 $\Delta$ sp-GFP than CLV3-GFP was present in protoplasts at 24h after transfection, the latter likely representing only the molecules synthesized during the last 1–2 h before homogenization (Fig. 2D). No secreted CLV3-GFP was detected (Fig. 2D, out; the very small

amount of CLV3 $\Delta$ sp-GFP in the incubation medium was most probably due to the unavoidable contamination by material from a small proportion of dead protoplasts). Consistently, microscopy showed clear fluorescence in protoplasts expressing CLV3 $\Delta$ sp-GFP, which also accumulated in the nucleus as often occurs when free GFP or its fusions with short polypeptides are expressed, but practically no fluorescence in those expressing CLV3-GFP (Fig. 3). Therefore, the instability detected by pulse-chase was confirmed by analysis of the CLV3-GFP steady-state accumulation.

### *3.2. CLV3-GFP degradation is not inhibited by brefeldin A or wortmannin*

To acquire information on the pathway followed by CLV3-GFP before its disappearance, perturbators of the biosynthetic secretory pathway were used. Wortmannin inhibits receptor-mediated protein sorting from the Golgi complex to vacuoles, causing default secretion of several vacuolar proteins [24]. The bean vacuolar storage protein phaseolin is cleaved into fragments corresponding approximately to half of the polypeptide upon sorting into the vacuole, but not when a mutated form is secreted [16,25] and was therefore used as a control. Wortmannin inhibited the vacuole-mediated fragmentation of phaseolin (Fig. 4A, asterisk indicates intact phaseolin, vertical bar indicates phaseolin fragments) but had no effect on the disappearance of CLV3-GFP (Fig. 4B). Brefeldin A (BFA) causes deregulated fusion of Golgi cisternae with the ER and inhibits further traffic of newly synthesized proteins, thus blocking both secretion and vacuolar sorting of proteins that traffic through the Golgi complex [14-16]. The drug thus inhibits secretion of mGFP5 and vacuolar delivery of a modified derivative with an added vacuolar sorting signal [14,15], as well as the vacuole-mediated, post-translational fragmentation of phaseolin [16]. The inhibition of phaseolin fragmentation by BFA can be visualized by pulse-chase (Fig. 4C and Fig. S2) and causes high accumulation of intact phaseolin detected by protein blot (Fig. 4A). Conversely, BFA did not alter CLV3-GFP stability apart from a slight stabilization at 1 h chase (Fig. 4D and Fig. S2).

It can be concluded that the disappearance of CLV3-GFP does not require Golgi-mediated delivery to the vacuole and seems to occur before traffic out of the ER, as also suggested by the observation that this disappearance is very rapid when compared to mGFP secretion (see Fig. 2B).

### *3.3. The active CLV3 peptide is produced in transgenic tobacco constitutively expressing CLV3-GFP*

To verify whether the CLV3-GFP degradation occurring in protoplasts indeed leads to the formation of the active CLV3 peptide, the fusion protein was expressed in transgenic tobacco under the 35S promoter. These transgenic plants grew normally, not showing any marked visible phenotype. Pulse-chase of protoplasts prepared from transgenic leaves indicated that newly synthesized CLV3-GFP rapidly disappeared, as upon transient expression (Fig. 5A). Even after very short pulse, no fragmentation products recognized by the anti-GFP antiserum could be detected (Fig. 5B).

When supplemented to the medium of growing Arabidopsis seedling, a chemically-synthesized dodecapeptide corresponding to the functional CLV3 dodecapeptide (RTVPSGPDPLHH, CLV3p12, [12]) causes the consumption of root meristems, resulting in shortened root length indicative of CLV3 activity [4,12,26]. The culture medium of CLV3-GFP transgenic tobacco protoplasts was therefore supplemented to germinating Arabidopsis seeds. After 10 days growth, a marked reduction in root length, compared to the untreated control, was clearly detectable (Fig. 5C) and comparable to that obtained by supplementing the CLV3p12 synthetic peptide to a final 50 nM concentration (Fig. 5D). Using a LC-MS/MS assay, we verified the presence of the expected CLV3 peptide in the culture medium of transgenic protoplasts. The identification was based on comparison of the corresponding CLV3p12 standard and the selected transition  $656,8 > 503,0$  (Fig. 5E).  $656,8$  m/z corresponds to the double charged standard ion  $(M+2H)^{2+}$ , and the  $503,0$  m/z product ion corresponds to the C-terminal fragment of the peptide  $(-P-L-H-H-COOH)$ , [4]. We conclude that expression

of CLV3-GFP in tobacco leaves leads to the secretion of the active CLV3 peptide.

#### *3.4. The stability of intact CLV3-GFP can be increased by inhibiting ER-associated protein degradation*

The results presented above suggest that the pathway producing the secreted CLV3 active peptide involves rapid disappearance of the intact precursor, unaffected by inhibitors of secretory traffic. These features are typical of ER-associated degradation (ERAD), which disposes of structurally defective secretory proteins, usually through retrotranslocation from the ER into the cytosol, ubiquitination and proteasomal degradation [27]. We therefore verified whether inhibitors of ERAD affect the disappearance of CLV3-GFP. Protoplasts from transgenic tobacco were subjected to pulse-chase in the absence or presence of the proteasomal inhibitor MG132. Already at the end of the pulse, a higher amount of newly synthesized CLV3-GFP was immunoselected from MG132-treated protoplasts (Fig. 6A). To verify whether the effect was protein-specific, the same treatments were performed on protoplasts expressing  $\Delta 418$  phaseolin, which is not an ERAD substrate [25]. MG132 caused a marked decrease of recovered  $\Delta 418$  phaseolin at the end of pulse (Fig 6B). This is consistent with the fact that in mammalian systems MG132 stabilizes ERAD substrates but also rapidly inhibits protein synthesis [28,29], and indicates that the partial stabilizing effect of MG132 on CLV3-GFP is specific. The progressive disappearance of CLV3-GFP during the chase was also partially inhibited by MG132 (Fig. 6C).

Given the results of biochemical analysis, we tested whether MG132 allowed us to visualize CLV3-GFP by microscopy. Analysis of intact tissues did not show any GFP fluorescence, neither in the meristem apex where CLV3 is naturally expressed nor in other cells (Fig. 7A, apex is indicated by the arrow). Very weak fluorescence occasionally detected in the GFP channel (for example, approximately at the centre and bottom right of the left panel in Fig. 7A) was due to autofluorescence of probably cell wall polymers, since it could not be photobleached. Fluorescence in transgenic

protoplasts was also below the limit of visualization, consistent with the results of transient expression shown in Fig. 3, and was also undetectable upon MG132 treatment (data not shown). However, immunofluorescence microscopy using anti-GFP antiserum allowed the detection of specific, faint punctate structures that markedly increased in number and intensity upon MG132 treatment (Fig. 7B), confirming that the proteasome inhibitor had a positive effect on CLV3-GFP stability. Double immunofluorescence with anti-GFP and anti-SEC21 (a Golgi marker; [30-32]) indicated that the structures containing CLV3-GFP were distinct from Golgi stacks (Fig. 7C). Subcellular fractionation by isopycnic gradient ultracentrifugation (Fig. 7D) showed co-fractionation of CLV3-GFP with the ER chaperone BiP [16], in subcellular fractions with the expected density for the ER [16]. It can be concluded that the punctate structures containing CLV3-GFP represent transient points of accumulation of the newly synthesized recombinant protein within the ER, possibly just before disposal by ERAD.

Usually, ERAD involves an ubiquitin-interacting AAA-ATPase, designated CDC48 [33]. CDC48 is part of a ternary complex that contributes to retrotranslocation from the ER lumen by pulling the defective proteins from the cytosolic face of the ER membrane translocation channel [34]. Protoplasts prepared from transgenic plants expressing CLV3-GFP, or  $\Delta$ 418 phaseolin as a control, were transiently transfected with the plasmid encoding wild type CDC48 (CDC48wt) or a mutated form (CDC48QQ) that impairs the retro-translocation process also in plant cells [19]. Twelve hours after transfection, protoplasts were pulse-labelled for 1 h before homogenization and immunoprecipitation. The mutated CDC48 did not affect the amount of newly synthesized  $\Delta$ 418, while it increased by about 25% that of CLV3-GFP (Fig. 8). Altogether, the results presented in Figures 6, 7 and 8 support a role of ERAD in the rapid disappearance of the CLV3 precursor.

We analysed the CLV3 sequence using the Pcleavage proteasome cleavage prediction program (Pcleavage: <http://www.imtech.res.in/raghava/pcleavage/>; [35]). Analysis based on in vitro constitutive proteasome data predicts cleavages that would generate the active CLV3 dodecapeptide, but also its further fragmentation at an



internal Val residue (Fig.S3A). Analysis based on MHC class I ligands predicts the formation of an 18-residue fragment containing the active CLV3 dodecapeptide (Fig.S3B).

### *3.5. Overexpression of endoplasmin specifically relieves the ER stress inhibition of CLV3-GFP synthesis*

The *shepherd* Arabidopsis mutant has greatly reduced levels of the HSP90 chaperone of the ER, endoplasmin (also termed glucose regulated protein 94, GRP94), because of a T-DNA insertion [18,36]. *Shepherd* has shoot and flower phenotypes that resemble those of loss of function mutants of CLV genes, in particular CLV3, and cannot be rescued by CLV3 overexpression [36], indicating that endoplasmin is directly or indirectly required for the activity of the CLV system.

We therefore verified whether a role of endoplasmin could be detected biochemically. The assay [21] measures the ability of putative molecular chaperones to alleviate the decrease in the synthesis of a given secretory protein occurring upon the ER stress imposed by tunicamycin (Tm), an inhibitor of N-glycosylation that causes a general inhibition of secretory protein synthesis, including those that are not glycoproteins [18,21]. The assay indicates that the overload of chaperone work, due to the folding defects in proteins that need to be glycosylated, causes a shortage of folding helpers within the ER that can be alleviated by chaperone overexpression [21]. We thus co-expressed CLV3-GFP, or control mGFP5, with either endoplasmin, barley  $\alpha$ -amylase (as a control secretory protein with no chaperone activity), or BiP. The latter is the heat shock 70 ER resident and a very promiscuous chaperone [37]. Endoplasmin is much more selective than BiP: a few newly synthesized animal proteins interacting with it have been identified [38,39], but to date potential plant clients have only been postulated based on yeast two-hybrid screening [40]. Overexpression of BiP or endoplasmin can be visualized by immunoprecipitation with the respective antisera from pulse-labelled protoplasts and shows that, upon transfection with equal amounts of

plasmid, BiP synthesis is increased in our system in a similar or slightly higher proportion than endoplasmin (Fig. 9A).

Tm inhibited the synthesis of CLV3-GFP or mGFP5 by 40-50% when these were co-expressed with  $\alpha$ -amylase (Fig. 9B). Endoplasmin fully abolished the Tm effect on CLV3-GFP (Fig. 9B, and 9C for quantitation). Endoplasmin action was stronger than that of BiP and synergistic to it (Fig. 9B and 9C). Its effect was quantitative (Fig. 9D). In the absence of Tm stress, when spare chaperone activity is presumably available, the effects of the chaperones were much more variable in independent experiments and a statistically significant ( $P < 0.05$ ) increase of CLV3-GFP synthesis was only observed when endoplasmin and BiP were co-overexpressed (Fig. 9E).

Considering that neither mGFP5 nor CLV3-GFP are glycoproteins, these results confirm previous work showing that the unfolded protein response does not fully rescue the increased general workload of folding helpers due to Tm action [18,21]. Most importantly, they indicate that endoplasmin specifically alleviates this phenomenon for a protein fusion in which the CLV3 sequence is added to GFP and that this effect is additive to that of BiP.

## 4. Discussion

### *4.1. Rapid intracellular processing of the CLAVATA3 precursor and a role of ER-associated protein degradation*

The biochemical and fluorescence microscopy results reported here indicate that CLV3 proteolytic processing starts very soon after synthesis. The two GFP fusions disappear faster than CLV3-FLAG, suggesting that the type of protein tag influences either the rate of full CLV3 maturation or that of initial proteolytic events that eliminate recognized epitopes. However, irrespectively of the appended tag, in all cases there was a rapid loss of immunoprecipitable fusion during the first hours of chase and no secreted intact CLV3 fusion was detected.

We do not know which steps of CLV3 processing occur intracellularly: a major drawback of studies performed on tagged proteins is that, if the tag is

lost by proteolytic processing, it is impossible to trace exactly the series of events that follow such an event. However, the results of BFA and wortmannin treatments, and the fact that the CLV3 active peptide is produced and found extracellularly, rule out the participation of the vacuole and suggest that processing occurs, or at least starts, without the involvement of post-ER compartments of the secretory pathway. By fluorescence microscopy, we have been virtually unable to detect signals from CLV3-GFP, consistent with the rapid disappearance of the intact protein observed by biochemical analysis. Immunocytochemistry detected faint punctate structures that were distinct from Golgi stacks and increased in number under MG132 treatment, thus possibly representing CLV3-GFP in the ER lumen or at ER-proteasome attachment sites [41]. Absence of the signal peptide stabilizes intact CLV3-GFP, indicating that synthesis by ER-bound polysomes, and therefore presumably translocation into the ER lumen, is necessary for processing. The protease SOL1, which is involved in CLE19 processing, is located in endosomes but not along the pathway to the vacuole [42]. Although this enzyme does not seem to be involved in CLV3 processing [42], the study confirms that processing of proteins of the CLE family can occur, at least in part, intracellularly.

The stabilizing effects of the proteasome inhibitor MG132 and the ERAD inhibitor CDC48QQ indicate that at least a relevant proportion of CLV3-GFP newly synthesized polypeptides is an ERAD substrate. The biological activity assay and the biochemical analysis of protoplast incubation medium indicate that expression of CLV3-GFP in transgenic tobacco allows the production of the active CLV3 peptide. Different possible models may explain these observations. ERAD could have a physiological role in modulating the amount of CLV3 precursor allowed to leave the ER to undergo extracellular maturation, and would thus regulate the production of active peptide. Similarly, the fraction GABA<sub>B</sub> receptors that reaches the cell surface in neurons is modulated by degradation of newly synthesized polypeptides by the ERAD machinery [43]. The amount of intact CLV3 precursor that reaches the cell surface would be extremely small in tobacco vegetative cells, but ERAD activity could be specifically regulated in meristematic cells to finely tune CLV3 production. Alternatively, ERAD may

have a direct role in producing the active CLV3 peptide, rather than disposing of precursors that will not produce it. This would be consistent with the prediction of consensus sites for proteasome cleavage compatible with the formation of the active dodecapeptide or a slightly larger peptide that could be further processed en route to secretion. Such a pathway to produce active CLV3 would open relevant questions regarding both the mechanism of secretion of the CLV3 peptide and the consistency of the results presented here with the available literature on CLV3. These remain now unresolved, probably also because to our best knowledge there are no other studies in which the intact CLV3 precursor or fusions containing it were biochemically detected by electrophoresis in plant cells, but we try below to define them in more detail.

#### *4.2. Consistency with known CLV3 biochemistry and cell biology*

The first two (out of three) Pro residues of the natural, active CLV3 peptide are hydroxylated to Hyp residues, the second Hyp being further modified by O-glycosylation with three arabinose residues [4,44]. These modifications are not strictly necessary for activity, but increase the interactions with the CLV3 receptors ([4,44]. Arabidopsis Prolyl-4-Hydroxylases occur in the ER and perhaps also in the Golgi apparatus [45]. Three hydroxyproline O-arabinosyltransferases have been localized to the Golgi apparatus [46]. Therefore, prolyl hydroxylation rapidly occurring in the ER after synthesis is compatible with CLV3 being an ERAD substrate, and actually the detection of one major polypeptide and additionally closely migrating ones after pulse-labelling suggests some form of processing. Arabinosylation seems instead to require passage through the Golgi apparatus, a trafficking step that does not usually occur before ERAD substrates are dislocated from the ER to the cytosol to be degraded by the proteasome. If proteasome processing is indeed along the route to the production of active CLV3, the product should therefore be translocated back into the secretory pathway to be O-glycosylated in the Golgi apparatus. Peptides generated by proteolysis in the cytosol can be translocated into the ER lumen as part of the animal major histocompatibility complex (MHC) class I antigen-processing pathway

[47]. This leads to peptide association to the MHC class I molecules and deliver of the complex to the cell surface via the Golgi apparatus, to be presented to cytotoxic lymphocytes. It is not known whether a mechanism to bring peptides from the cytosol into the ER exists in plant cells. Alternatively, after ERAD-mediated dislocation of CLV3 from the ER to the cytosol and degradation by the proteasome, the resulting, active CLV3 peptide could follow one of the unconventional secretion pathways, which do not involve traffic through the ER and Golgi apparatus [48]: some plant O-glycosylation enzymes have also been localized in compartments involved in unconventional secretion [49]. A role of ERAD in the pathway to form active CLV3 could be relevant for explaining the involvement of the E3 ubiquitin ligase PUB4 in CLV3 signalling in root meristems [50], a finding defined by the authors as a “mystery in genetics” [51].

When fusions between GFP and either CLV3 or other proteins of the CLE family under constitutive promoter were expressed in transgenic plants or transiently transformed epidermal cells, microscopy revealed fluorescence at the cell surface, consistent with secretion [7,52]. T7-tagged CLV3 constructs expected to be secreted were also detected in the apoplast by immunoelectron microscopy of roots, but when the addition of a vacuolar sorting peptide mutated them, they became undetectable and only marginally produced the typical phenotypes of CLV3 overexpression [7]. We hypothesize that the discrepancy with respect to our inability to detect any secreted intact CLV3 fusion could be only apparent, since microscopy does not provide information on the actual relative proportion of molecules that reach the cell surface as intact polypeptides. As we discussed above, this could be a very small fraction of newly synthesized CLV3-GFP, accumulating at levels detectable by fluorescence in certain tissues but below the limits of detection in the systems we have used, and could be not representative of the bulk of precursor that actually generates the peptide. Consistent with our results, a CLV3-YFP fusion transiently expressed in *Nicotiana benthamiana* is biochemically active but is barely detectable by protein blot when compared to control YFP expressed under the same promoter [53]. The inhibitory effect of the addition of a vacuolar sorting peptide on secretion and activity could result from a dominant effect of the

vacuolar sorting signal. Although most plant soluble proteins are separated from those destined for secretion in the Golgi apparatus or trans-Golgi network, growing evidence indicates that the physical recognition of vacuolar sorting signals occurs already in the ER [54]. This sorting event could inhibit the dislocation of CLV3 fusions from the ER into the cytosol.

When expressed in the plant secretory pathway, GFP detectable after pulse-labelling is usually rather stable during subsequent chase, independently of whether it is modified for ER retention, secretion or vacuolar sorting [15,55]. When fused to sequences that lead to delivery to the vacuole, the GFP “core” is often released from the fusion proteins, most probably because GFP contains a protease-sensitive site, but this core remains detectable and can be immunoprecipitated with anti-GFP antisera [15,24,55]. The core is however not detectable as a degradation product of an unstable secretory GFP fusion most probably delivered to the cytosol by ERAD [56]. The stability of GFP has also been markedly reduced by the addition of short sequences that target proteins for rapid proteolysis, such as the PEST sequences [57,58]. Our data indicate that the addition of CLV3 similarly alters the stability of GFP. This destabilizing activity may be suggestive of an intrinsically disordered state of the CLV3 precursor, a feature that may make it a substrate for ERAD and/or favour very rapid processing.

#### *4.3. A possible role of endoplasmin*

We have shown that endoplasmin supports CLV3-GFP synthesis under ER stress. The effect is stronger than that of BiP, and the actions of the two chaperones are additive. When  $\alpha$ -amylase had been tested in the same assay, endoplasmin was less effective than BiP [18]. These findings point to endoplasmin as a specific key player in the synthesis of a protein involved in meristem functions and provide a first, possible biochemical explanation for the observed genetic relationships between endoplasmin and the CLAVATA system [36].

Endoplasmin is absent from most unicellular organisms; its complete knockdown is compatible with mammalian cell survival in culture but is

embryo-lethal, indicating that basic activities of the secretory pathway can dispose of this chaperone but certain functions essential for the establishment of specific tissue developments require it [38]. Endoplasmin has also peptide binding properties distinct from its chaperone activity [59], a characteristic that, together with immunology data on tumors [60], has involved endoplasmin in antigenic peptide presentation, although the evidence remains controversial [61,62]. BiP recognizes short peptide sequences enriched in bulk hydrophobic amino acids, expected to be masked by correct protein folding and assembly [63-65]. The recognition properties of endoplasmin, and of HSP90 in general, are less easily defined. HSP90 clients do not have clearly identifiable sequence or hydrophobicity features, but they have higher thermal instability than non-clients [66]. The assay used here does not necessarily imply a direct interaction between endoplasmin and CLV3-GFP. However, the observation that CLV3-GFP is functional but also a particularly unstable protein is in agreement with the characteristics of HSP90 clients defined above.

In summary, the *in vivo* biochemical analysis of CLV3 synthesis reported here point to very rapid intracellular processing events in early compartments of the secretory pathway and a specific role of ERAD and endoplasmin, the latter possibly related to recognition properties towards unstable polypeptides.

### **Conflict of interest statement**

Conflicts of interest: none.

### **Acknowledgements**

We thank Jennifer Fletcher for the CLV3-GFP and CLV3 $\Delta$ sp-GFP DNA constructs, Alex Costa and the microscope imaging facility UNITECH NOLIMITS of the University of Milan for confocal microscopy analyses, Aldo Ceriotti for the CDC48 constructs, and Chun-Ming Liu for the CLV3p12 peptide. We also thank Adriana Carino and Francesc Jmenez for technical assistance, and Emanuela Pedrazzini for the stimulating discussions. Work

supported in part by the EU Research Training Network “Biochemical and genetic approaches to study bio-molecular interactions in plants” (HPRN-CT-2002-00262) and MIUR-FIRB Project RBNE01TYZF.

## **Appendix A. Supplementary data**

Fig. S1. Intact CLV3-mGFP5 rapidly disappears in Arabidopsis protoplasts.

Fig. S2. Quantitative analysis of the effects of BFA on CLV3.-GFP and phaseolin stability.

Fig. S3. Prediction of proteasome cleavage sites in the CLV3 sequence.

## **References**

- [1] J.C. Fletcher, U. Brand, M.P. Running, R. Simon, E.M. Meyerowitz, Signaling of cell fate decisions by CLAVATA3 in Arabidopsis shoot meristems. *Science* 283 (1999) 1911–1914.
- [2] J.H. Jun, E. Fiume, J.C. Fletcher, The CLE family of plant polypeptide signalling molecules. *Cell. Mol. Life Sci.* 65 (2008) 743-755.
- [3] R. Tabata, S. Sawa, Maturation processes and structures of small secreted peptides in plants. *Front. Plant Sci.* 5 (2014) 311.
- [4] T. Kondo, S. Sawa, A. Kinoshita, S. Mizuno, T. Kakimoto, H. Fukuda, Y. Sakagami, A plant peptide encoded by CLV3 identified by in situ MALDI TOF-MS analysis. *Science* 313 (2006) 845-848.
- [5] M. Ogawa, H. Shinohara, Y. Sakagami, Y. Matsubayashi, Arabidopsis CLV3 peptide directly binds CLV1 ectodomain. *Science* 319 (2008) 294.
- [6] H. Shinohara, Y. Matsubayashi, Reevaluation of the CLV3-receptor interaction in the shoot apical meristem: dissection of the CLV3 signalling pathway from a direct ligand-binding point of view. *Plant J.* 82 (2015) 328–336.



- [7] E. Rojo, V.K. Sharma, V. Kovaleva, N.V. Raikhel, J.C. Fletcher, CLV3 is localized to the extracellular space, where it activates the Arabidopsis CLAVATA stem cell signalling pathway. *Plant Cell* 14 (2002) 969–977.
- [8] M. Lenhard, T. Laux, Stem cell homeostasis in the Arabidopsis shoot meristem is regulated by intercellular movement of CLAVATA3 and its sequestration by CLAVATA1. *Development* 130 (2003) 3163–3173.
- [9] J. Ni, S.E. Clark, Evidence for functional conservation, sufficiency, and proteolytic processing of the CLAVATA3 CLE Domain. *Plant Physiol.* 140 (2006) 726–733.
- [10] J. Ni, Y. Guo, H. Jin, J. Hartsell, S.E. Clark, Characterization of a CLE processing activity. *Plant Mol. Biol.* 75 (2011) 67–75.
- [11] T. Tamaki, S. Betsuyaku, M. Fujiwara, Y. Fukao, H. Fukuda, S. Sawa, SUPPRESSOR OF LLP1 1-mediated C-terminal processing is critical for CLE19 peptide activity. *Plant J.* 76 (2013) 970–981.
- [12] T.T. Xu, X.F. Song, S.C. Ren, C.M. Liu, The sequence flanking the N-terminus of the CLV3 peptide is critical for its cleavage and activity in stem cell regulation in Arabidopsis. *BMC Plant Biol.* 13 (2013) 225.
- [13] R.P. Hellens, E.A. Edwards, N.R. Leyland, S. Bean, P.M. Mullineaux, pGreen: a versatile and flexible binary Ti vector for Agrobacterium mediated plant transformation. *Plant Mol. Biol.* 42 (2000) 819–832.
- [14] A. Pompa, F. De Marchis, A. Vitale, S. Arcioni, M. Bellucci, An engineered C-terminal disulfide bond can partially replace the phaseolin vacuolar sorting signal. *Plant J.* 61, (2010) 782–791.
- [15] L. Frigerio, O. Foresti, D. Hernández Felipe, J-M. Neuhaus, A. Vitale, The C-terminal tetrapeptide of phaseolin is sufficient to target green fluorescent protein to the vacuole. *J. Plant Physiol.* 158 (2001) 499–503.
- [16] E. Pedrazzini, G. Giovinazzo, A. Bielli, M. de Virgilio, L. Frigerio, M. Pesca, F. Faoro, R. Bollini, A. Ceriotti, A. Vitale, Protein quality control along the route to the plant vacuole. *Plant Cell* 9 (1997) 1869–1880.

- [17] K.R. Siemering, R. Golbik, R. Sever, J. Haseloff, Mutations that suppress the thermosensitivity of green fluorescent protein. *Curr. Biol.* 6 (1996) 1653-1663.
- [18] E.M. Klein, L. Mascheroni, A. Pompa, L. Ragni, T. Weimar, K.S. Lilley, P. Dupree, A. Vitale, Plant endoplasmic reticulum supports the protein secretory pathway and has a role in proliferating tissues. *Plant J.* 48 (2006) 657-673.
- [19] R.S. Marshall, N.A. Jolliffe, A. Ceriotti, C.J. Snowden, J.M. Lord, L. Frigerio, L.M. Roberts, The role of CDC48 in the retro-translocation of non-ubiquitinated toxin substrates in plant cells. *J. Biol. Chem.* 283 (2008) 15869–15877.
- [20] M. de Virgilio, F. De Marchis, M. Bellucci, D. Mainieri, M. Rossi, E. Benvenuto, S. Arcioni, A. Vitale, The human immunodeficiency virus antigen Nef forms protein bodies in leaves of transgenic tobacco when fused to zeolin. *J. Exp. Bot.* 10 (2008) 2815–2829.
- [21] N. Leborgne-Castel, E.P.W.M. Jelitto-Van Dooren, A. J. Crofts, J. Denecke, Overexpression of BiP in tobacco alleviates endoplasmic reticulum stress. *Plant Cell* 11 (1999) 459–469.
- [22] F. De Marchis, M. Bellucci, A. Pompa, Traffic of human  $\alpha$ -mannosidase in plant cells suggests the presence of a new Endoplasmic Reticulum-to-Vacuole pathway without involving the Golgi complex. *Plant Physiol.* 161 (2013) 1769-1782.
- [23] X. Zhang, R. Henriques, S.S. Lin, Q.W. Niu, N.H. Chua, Agrobacterium-mediated transformation of *Arabidopsis thaliana* using the floral dip method. *Nat. Protoc.* 1 (2006) 641-646.
- [24] L.L. DaSilva, J.P. Taylor, J.L. Hadlington, S.L. Hanton, C.J. Snowden, S.J. Fox, O. Foresti, F. Brandizzi, J. Denecke, Receptor salvage from the prevacuolar compartment is essential for efficient vacuolar protein targeting. *Plant Cell* 17 (2005) 132–148.

- [25] L. Frigerio, M. de Virgilio, A. Prada, F. Faoro, A. Vitale, Sorting of phaseolin to the vacuole is saturable and requires a short C-terminal peptide. *Plant Cell* 10 (1998) 1031–1042.
- [26] A. Kinoshita, S. Betsuyaku, Y. Osakabe, S. Mizuno, S. Nagawa, Y. Stahl, R. Simon, K. Yamaguchi-Shinozaki, H. Fukuda, S. Sawa, RPK2 is an essential receptor-like kinase that transmits the CLV3 signal in *Arabidopsis*. *Development* 137 (2010) 3911–3920.
- [27] T. Anelli, R. Sitia, Physiology and pathology of proteostasis in the early secretory compartment. *Semin. Cell Dev. Biol.* 21 (2010) 520–525
- [28] J.L. Cowan, S.J. Morley, The proteasome inhibitor, MG132, promotes the reprogramming of translation in C2C12 myoblasts and facilitates the association of hsp25 with the eIF4F complex. *Eur. J. Biochem.* 271 (2004) 3596–3611.
- [29] A. Yerlikaya, S.R. Kimbal, B.A. Stanley, Phosphorylation of eIF2 $\alpha$  in response to 26S proteasome inhibition is mediated by the haem-regulated inhibitor (HRI) kinase. *Biochem. J.* 412 (2008) 579–588.
- [30] A. Movafeghi, N. Happel, P. Pimpl, G.H. Tai, D.G. Robinson, *Arabidopsis* Sec21p and Sec23p homologs. Probable coat proteins of plant COP-coated vesicles. *Plant Physiol.* 119 (1999) 1437–1446.
- [31] P. Pimpl, A. Movafeghi, S. Coughlan, J. Denecke, S. Hillmer, D.G. Robinson, In situ localization and in vitro Induction of plant COPI-coated vesicles. *Plant Cell* 12 (2000) 2219–2235.
- [32] A.J. Groen, G. Sancho-Andrés, L.M. Breckels, L. Gatto, F. Aniento, K.S. Lilley, Identification of trans-Golgi network proteins in *Arabidopsis thaliana* root tissue. *J. Proteom. Res.* 13 (2014) 763–776.
- [33] D.H. Wolf, A. Stolz, The Cdc48 machine in endoplasmic reticulum associated protein degradation. *Biochim. . Biophys. Acta* 1823 (2012) 117–124.
- [34] Y.H. Ye, H.H. Meyer, T.A. Rapoport, The AAA ATPase Cdc48/p97 and its partners transport proteins from the ER into the cytosol. *Nature* 414 (2001) 652–656.

- [35] M. Bhasin, G.P. Raghava, Pcleavage: an SVM based method for prediction of constitutive proteasome and immunoproteasome cleavage sites in antigenic sequences. *Nucleic Acids Res.* 33 (2005) W202-W207.
- [36] S. Ishiguro, Y. Watanabe, N. Ito, H., Nonaka, N. Takeda, T. Sakai, H. Kanaya, K. Okada, SHEPHERD is the Arabidopsis GRP94 responsible for the formation of functional CLAVATA proteins. *EMBO J.* 21 (2002) 898-908.
- [37] A. Vitale, R.S. Boston, Endoplasmic reticulum quality control and the unfolded protein response: insights from plants. *Traffic* 9 (2008) 1581–1588.
- [38] M. Marzec, D. Eletto, Y. Argon, GRP94: An HSP90-like protein specialized for protein folding and quality control in the endoplasmic reticulum. *Biochim. Biophys. Acta* 1823 (2012) 774-787.
- [39] B. Liu, M. Staron, F. Hon, B.X. Wu, S. Sun, C. Morales, C.E. Crosson, S. Tomlinson, D. Kim Wu, Z. Li, Essential roles of grp94 in gut homeostasis via chaperoning canonical Wnt pathway *Proc. Natl. Acad. Sci. USA* 110 (2013) 6877-6882.
- [40] L.P. Chong, Y. Wang, N. Gad, N. Anderson, B. Shah, R. Zhao, A highly charged region in the middle domain of plant endoplasmic reticulum (ER)-localized heat-shock protein 90 is required for resistance to tunicamycin or high calcium-induced ER stresses. *J. Exp. Bot.* 66 (2015) 113-124.
- [41] W. Ng, T. Sergeyenko, N. Zeng, J.D. Brown, K. Römisch, Characterization of the proteasome interaction with the Sec61 channel in the endoplasmic reticulum. *J. Cell Sci.* 120 (2007) 682-691.
- [42] T. Tamaki, S. Betsuyaku, M. Fujiwara, Y. Fukao, H. Fukuda, S. Sawa, SUPPRESSOR OF LLP1 1-mediated C-terminal processing is critical for CLE19 peptide activity. *Plant J* 76 (2013) 970-981.
- [43] K. Zemoura, M. Schenkel, M.A. Acuna, G.E. Yevenes, H.U. Zeilhofer, D. Benke, Endoplasmic reticulum-associated degradation controls cell

- surface expression of  $\gamma$ -aminobutyric acid, type B receptors. *J. Biol. Chem.* 288 (2013) 34897–34905.
- [44] K. Ohyama, H. Shinohara, M. Ogawa-Ohnishi, Y. Matsubayashi, A glycopeptide regulating stem cell fate in *Arabidopsis thaliana*. *Nat. Chem. Biol.* 5 (2009) 578–580.
- [45] S.M. Velasquez, M.M. Ricardi, C.P. Poulsen, A. Oikawa, A. Dilokpimol, A. Halim, S. Mangano, S.P.D. Juarez, E. Marzol, J.D.S. Salter, et al., Complex regulation of Prolyl-4-hydroxylases impacts root hair expansion. *Mol. Plant* 8 (2015) 734–746.
- [46] M. Ogawa-Ohnishi, W. Matsushita, Y. Matsubayashi, Identification of three hydroxyproline O-arabinosyltransferases in *Arabidopsis thaliana*. *Nat. Chem. Biol.* 9 (2013) 726–730.
- [47] M. Del Val, S. Iborra, M. Ramos, S. Lázaro, Generation of MHC class I ligands in the secretory and vesicular pathways. *Cell. Mol. Life Sci.* 68, (2011) 1543–1552.
- [48] D.G. Robinson, Y. Ding, L.W. Jiang, Unconventional protein secretion in plants: a critical assessment. *Protoplasma* 253 (2016) 31–43.
- [49] C.P. Poulsen, A. Dilokpimol, G. Mouille, M. Burow, N. Geshi, Arabinogalactan glycosyltransferases target to a unique subcellular compartment that may function in unconventional secretion in plants. *Traffic* 15 (2014) 1219–1234.
- [50] Kinoshita, C.A. Ten Hove, R. Tabata, M. Yamada, N. Shimizu, T. Ishida, K. Yamaguchi, S. Shigenobu, Y. Takebayashi, S. Iuchi, et al., A plant U-box protein, PUB4, regulates asymmetric cell division and cell proliferation in the root meristem. *Development* 142 (2015) 444–453.
- [51] Kinoshita, M. Seo, Y. Kamiya, S. Sawa, Mystery in genetics: PUB4 gives a clue to the complex mechanism of CLV signalling pathway in the shoot apical meristem. *Plant Sign. Behav.* 10 (2015) e1028707.
- [52] V.K. Sharma, J. Ramirez, J.C. Fletcher, The *Arabidopsis* CLV3-like (CLE) genes are expressed in diverse tissues and encode secreted proteins. *Plant Mol. Biol.* 51 (2003) 415–425.

- [53] S. Betsuyaku, F. Takahashi, A. Kinoshita, H. Miwa, K. Shinozaki, H. Fukuda, S. Sawa, Mitogen-activated protein kinase regulated by the CLAVATA receptors contributes to shoot apical meristem homeostasis. *Plant Cell Physiol.* 52 (2011) 14–29.
- [54] D.G. Robinson, J-M. Neuhaus, Receptor-mediated sorting of soluble vacuolar proteins: myths, facts, and a new model. *J. Exp. Bot.* 67 (2016) 4435-4449.
- [55] O. Foresti, F. De Marchis, M. de Virgilio, E.M. Klein, S. Arcioni, M. Bellucci, A. Vitale, Protein domains involved in assembly in the endoplasmic reticulum promote vacuolar delivery when fused to secretory GFP, indicating a protein quality control pathway for degradation in the plant vacuole. *Mol. Plant* 1, (2008) 1067-1076.
- [56] F. Brandizzi, S. Hanton, L.L. DaSilva, P. Boevink, D. Evans, K. Oparka, J. Denecke, C. Hawes, ER quality control can lead to retrograde transport from the ER lumen to the cytosol and the nucleoplasm in plants. *Plant J.* 34 (2003) 269–281.
- [57] X. Li, X. Zhao, Y. Fang, X. Jiang, T. Duong, C. Fan, C-C. Huang, S.R. Kain, Generation of destabilized green fluorescent protein as a transcription reporter. *J. Biol. Chem.* 273 (1998) 34970–34975.
- [58] C. Mateus, S.V. Avery, Destabilized green fluorescent protein for monitoring dynamic changes in yeast gene expression with flow cytometry. *Yeast* 16 (2000) 1313–1323.
- [59] O. Ostrovsky, C.A. Makarewich, E.L. Snapp, Y. Argon, An essential role for ATP binding and hydrolysis in the chaperone activity of GRP94 in cells. *Proc. Natl. Acad. Sci. USA* 106 (2009) 11600-11605.
- [60] R. Suto, P.K. Srivastava, A mechanism for the specific immunogenicity of heat shock protein-chaperoned peptides. *Science* 269 (1995) 1585-1588.
- [61] R. Demine, P. Walden, Testing the role of gp96 as peptide chaperone in antigen processing. *J. Biol. Chem.* 280 (2005) 17573–17578.

- [62] A.R. Jockheck-Clark, E.V. Bowers, M.B. Totonchy, J. Neubauer, S.V. Pizzo, C.V. Nicchitta, Re-examination of CD91 function in GRP94 (Glycoprotein 96) surface binding, uptake, and peptide cross-presentation. *J Immunol.* 185 (2010) 6819-6830.
- [63] G.C. Flynn, J. Pohl, M.T. Flocco, J.E. Rothman, Peptide-binding specificity of the molecular chaperone BiP. *Nature* 353 (1991) 726-730.
- [64] S. Blond-Elguindi, S.E. Cwirla, W.J. Dower, R.J. Lipshutz, S.R. Sprang, J.F. Sambrook, M.J. Gething, Affinity panning of a library of peptides displayed on bacteriophages reveals the binding specificity of BiP. *Cell* 75 (1993) 717-728.
- [65] O. Foresti, L. Frigerio, H. Holkeri, M. de Virgilio, S. Vavassori, A. Vitale, A phaseolin domain involved directly in trimer assembly is a determinant for binding by the chaperone BiP. *Plant Cell* 15 (2003) 2464-2475.
- [66] M. Taipale, I. Krykbaeva, M. Koeva, C. Kayatekin, K.D. Westover, G.I. Karras, S. Lindquist, Quantitative analysis of Hsp90-Client interactions reveals principles of substrate recognition. *Cell* 150 (2012) 987-1001.

## Figure legends

**Fig. 1.** CLV3 fusions introduced into the secretory pathway disappear intracellularly. Tobacco leaf protoplasts were transformed with plasmids encoding the proteins indicated in each panel or empty plasmid (Co). After pulse-labelling for 1 h with [<sup>35</sup>S]Met and [<sup>35</sup>S]Cys, chase was performed for the indicated h, except panel A, which was pulse-labelling only. Protoplast homogenates or, in panels B, C and D, homogenates of protoplasts (in) and their incubation medium (out) were immunoselected with anti-GFP serum. After SDS-PAGE, radioactive proteins were detected. (E) Quantitation of radioactive CLV3-FLAG or CLV3-GFP at different chase points in two fully independent transfections and labelling experiments. In panels A-D, the positions of molecular mass markers (in kD) are shown at right. In panel A, the two images are derived from the same gel and same exposure, after removal of irrelevant lanes. In panel B, the two images derive from two different experiments. In panel D, the two images represent different gels exposed for the same time, from the same expression, labelling and immunoprecipitation experiment using the same number of protoplasts.

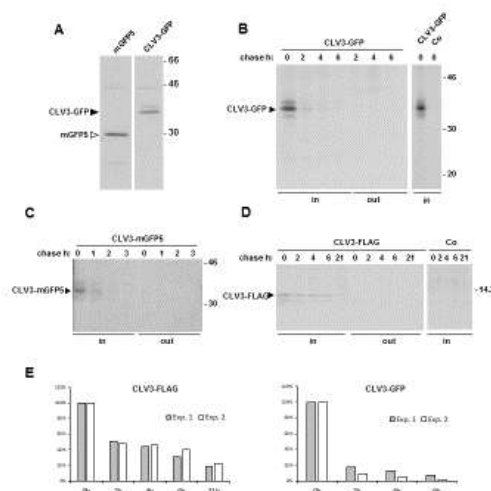


Figure 1



**Fig. 2.** CLV3-GFP does not perturb protein secretion and is stable when expressed in the cytosol. Tobacco leaf protoplasts were transformed with plasmids encoding the proteins indicated in each panel. A-C: after pulse-labelling for 1 h, chase was performed for the indicated h. Protoplast homogenates or, in panels A and B, homogenates of protoplasts (in) and their incubation medium (out) were immunoselected with anti-GFP serum. After SDS-PAGE, radioactive proteins were detected. (D) Protoplasts were transfected with plasmids encoding the indicated proteins or empty plasmid (Co). After incubation for 24 h, protoplasts (in) or incubation medium (out) were analysed by SDS-PAGE and protein blot with anti-GFP serum. As a loading control, Ponceau S staining is also shown (bottom). Quantitation of CLV3 $\Delta$ sp-GFP or CLV3-GFP in two fully independent protoplast transfections and protein blots is shown at right. In panels A-D, the positions of molecular mass markers (in kD) are shown at right.

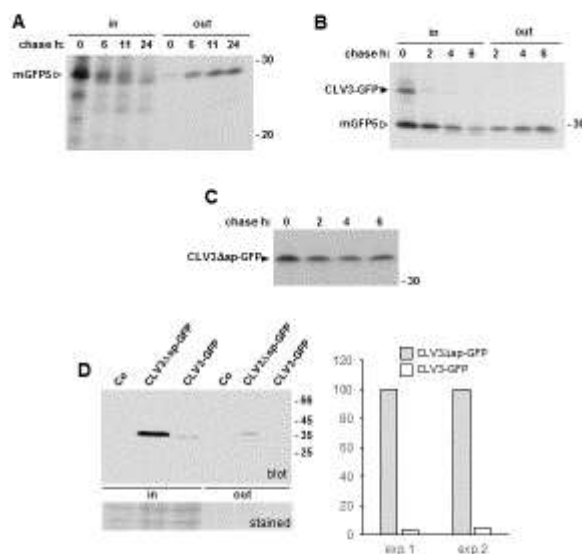


Figure 2

**Fig. 3.** Fluorescence of CLV3-GFP is almost undetectable in protoplasts. Tobacco leaf protoplasts were transfected with plasmids encoding CLV3-GFP or CLV3 $\Delta$ sp-GFP. After 24 h incubation, fluorescence of GFP or chloroplasts (Chl) was detected by epifluorescence microscopy. Two representative fields are shown for each transformation.

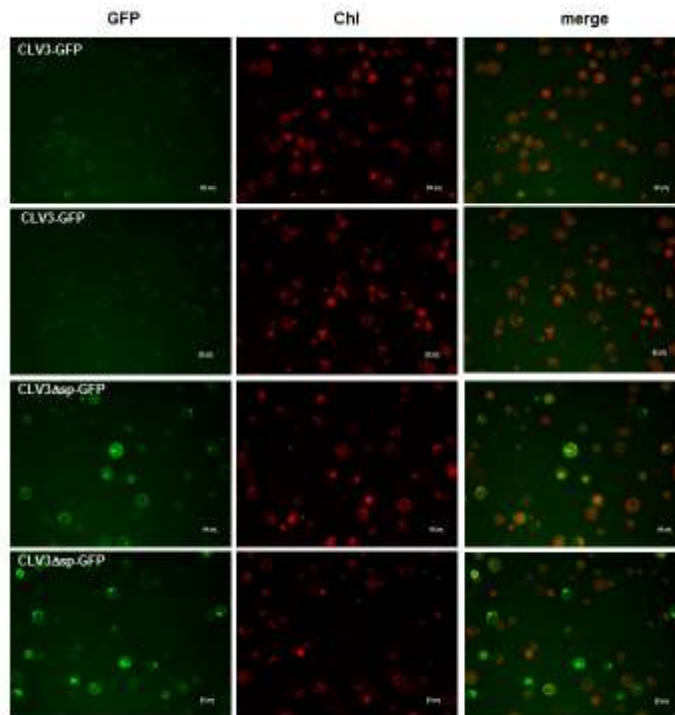


Figure 3

**Fig. 4.** Perturbators of the secretory pathway do not affect the stability of intact CLV3-GFP. Tobacco leaf protoplasts were transformed with plasmids encoding the proteins indicated in each panel or empty plasmid (Co). (A) After transformation, treatments were performed with (+) or without (-) BFA or wortmannin (wort) for 24 h before analysis of protoplast homogenates by SDS-PAGE and protein blot with anti-phaseolin serum (top). As a loading control, Ponceau S staining is also shown (bottom). (B) After pulse-labelling for 1 h, chase was for the indicated h. When indicated, the experiment was performed in the presence of wortmannin (wort). Homogenates of protoplasts (in) or their incubation medium (out) were immunoselected with anti-GFP serum and analysed by SDS-PAGE followed by detection of radioactive proteins. (C) and (D) Pulse and chase were performed with (+) or without (-) BFA, the homogenates immunoselected with anti-phaseolin (C) or anti-GFP (D) serum and proteins analysed as in (B). The positions of CLV3-GFP (arrowhead), intact phaseolin (asterisk) and phaseolin fragments (vertical bar) are indicated. In each panel, the positions of molecular mass markers (in kD) are shown at right.

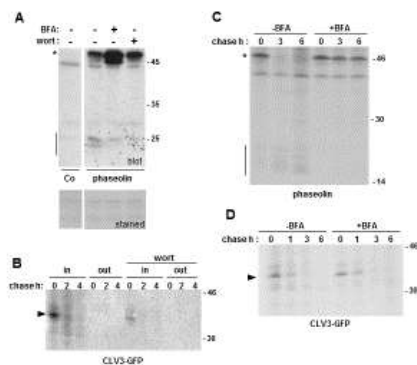


Figure 4

**Fig. 5.** Active CLV3 peptide is produced in transgenic tobacco constitutively expressing CLV3-GFP. (A) Protoplasts prepared from leaves of transgenic tobacco constitutively expressing CLV3-GFP or wt tobacco were pulse-labelled for 1 h and subjected to chase for the indicated h. Homogenates of protoplasts (in) and their incubation medium (out) were immunoselected with anti-GFP serum and analysed by SDS-PAGE and fluorography. (B) as in (A), but pulse was performed for only 15 or 30 min. Notice that 15 min pulse allows for only very low radioactive labelling. (C) Average root lengths of 10-d-old *A. thaliana* seedlings (n = 40) after seeding on MS supplemented with incubation medium of protoplasts from wt tobacco or transgenic tobacco expressing CLV3-GFP, and representative images of the experiment. (D) Measurements as in panel A, but MS was supplemented (+clv3p) or not (-clv3p) with the synthetic clv3p peptide. In C and D: error bar =  $\pm$  SD (three independent biological replicates); average root lengths with significant differences from the relative control are marked by the asterisk ( $P < 0.0001$  by Student's t-test). (E) LC-MS/MS chromatograms of the 656,8 > 503,0 transition of the CLV3p12 dodecapeptide (standard) and the medium of protoplasts isolated from leaves of wt tobacco or transgenic tobacco expressing CLV3-GFP. In (A) and (B), the positions of the proteins of interest are indicated at left and those of molecular mass markers (in kD) are shown at right.

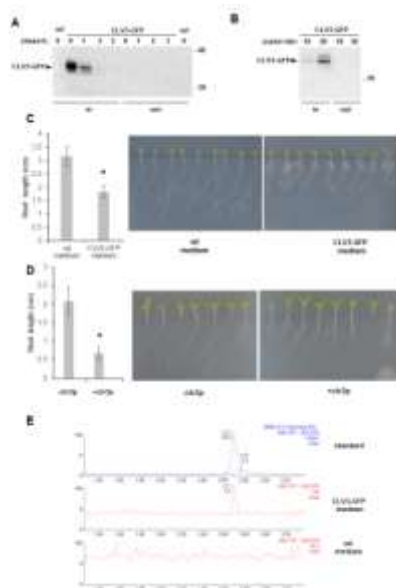


Figure 5

**Fig. 6.** The proteasome inhibitor MG132 increases CLV3-GFP stability. (A) Protoplasts isolated from leaves of wt tobacco (Co) or transgenic tobacco expressing CLV3-GFP were incubated in the presence or absence of MG132 and pulse-labelled for 1 h. Protoplast homogenates were immunoselected with anti-GFP serum and analysed by SDS-PAGE and fluorography. The graph at right shows, for two fully independent experiments, the relative intensity of radioactive bands, setting the value in the absence of MG132 to 100%. (B) Protoplasts isolated from leaves of transgenic tobacco expressing  $\Delta 418$  phaseolin were incubated in the presence or absence of MG132 and pulse-labelled for 1 h. Protoplast homogenates were immunoselected with anti-phaseolin serum and analysed by SDS-PAGE and fluorography. (C) Pulse-chase of transgenic tobacco protoplast expressing CLV3-GFP. Homogenates (in) and protoplast incubation medium (out) were immunoselected with anti-GFP anti-serum and analysed by SDS-PAGE and fluorography. The graph at right reports quantitation of radioactive bands representing CLV3-GFP in three fully independent experiments, setting the values at 0h chase to 100%; error bar =  $\pm$  SD. The positions of SDS-PAGE molecular mass markers (in kD) are indicated at left of the gel images.

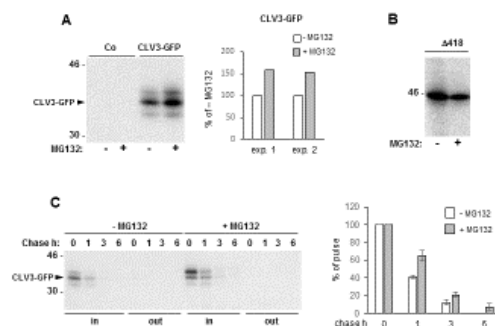


Figure 6

**Fig. 7.** CLV3-GFP detectable in transgenic tobacco is in the ER. (A) shoot apex of transgenic tobacco expressing CLV3-GFP was analyzed by confocal laser scanning microscopy. Left: GFP channel, green; centre: chlorophyll autofluorescence, blue; right: brightfield. In each panel, the arrow points to the shoot meristem apex. (B) Transgenic protoplasts expressing CLV3-GFP, or wt protoplasts (Co) were incubated in the presence or absence of MG132, fixed, incubated with anti-GFP antiserum and secondary FITC-conjugated antibody, and analysed for FITC fluorescence. (C) Transgenic protoplasts expressing CLV3-GFP were incubated with mouse anti-GFP and rabbit anti-SEC21 sera and then with the respective Texas Red- or FITC-conjugated secondary antibodies. Nuclei were stained with DAPI. The two images at bottom show controls without primary antisera. (D) Transgenic leaves expressing CLV3-GFP were homogenized in the presence of 12% (w/w) sucrose and absence of detergent. The homogenates were fractionated by ultracentrifugation on isopycnic sucrose gradient. Proteins in each gradient fraction were analyzed by SDS-PAGE and protein blot, with anti-GFP (upper image) or anti-BiP (bottom image) serum. Top of gradients is at left. Numbers at top indicate density ( $\text{g ml}^{-1}$ ).

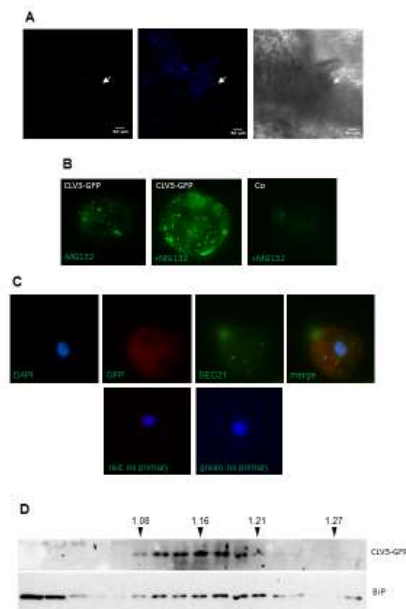


Figure 7

**Fig. 8.** CDC48QQ increases CLV3-GFP stability. Protoplasts prepared from leaves of transgenic tobacco expressing CLV3-GFP or  $\Delta 418$  phaseolin were co-transfected with plasmids encoding CDC48wt or CDC48QQ. After pulse-labelling for 1 h with [ $^{35}$ S]Met and [ $^{35}$ S]Cys, protoplast homogenates were immunoselected with anti-GFP (CLV3-GFP) or anti-phaseolin ( $\Delta 418$ ) serum and analysed by SDS-PAGE and fluorography. For CLV3-GFP, the two images are derived from the same gel and same exposure, after removal of irrelevant lanes. The graphs show the average values of the densitometry analysis from three independent experiments. Error bar =  $\pm$  SD

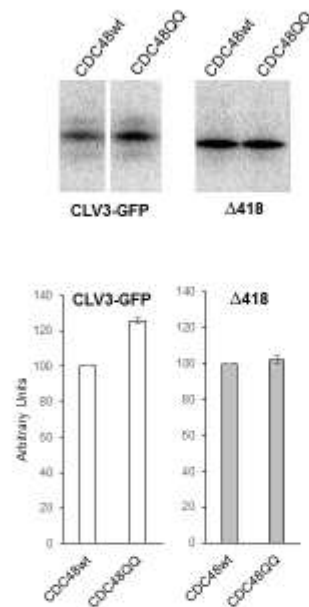


Figure 8

**Fig. 9.** Endoplasmic reticulum supports the synthesis of CLV3-GFP under ER-stress. In all panels, tobacco leaf protoplasts transiently transformed with plasmids encoding the indicated proteins were pulse-labelled with [<sup>35</sup>S]Met and [<sup>35</sup>S]Cys for 1h. Proteins were then immunoselected from protoplast homogenates using the appropriate antisera and analysed by SDS-PAGE and fluorography. (A) Protoplasts were co-transformed with plasmids encoding CLV3-GFP and either of the proteins indicated at top. Immunoselection was with anti-endoplasmic reticulum (top panel) or anti-BiP (bottom panel) antiserum. (B) Protoplasts were co-transformed with plasmids encoding CLV3-GFP (top image, filled arrowhead) or mGFP5 (bottom image, empty arrowhead) and either of the proteins indicated at top, and then pulse-labelled in the absence (-) or presence (+) of tunicamycin (Tm). Immunoselection was with anti-GFP antiserum. In panels A and B numbers at right indicate the positions of molecular mass markers, in kD. All samples in each of the four images were immunoselected from equal amounts of protoplasts. (C) Protoplasts were co-transformed with plasmids encoding mGFP5 or CLV3-GFP and either of the proteins indicated at bottom. Immunoprecipitation was with anti-GFP antiserum. After SDS-PAGE and fluorography, the intensity of the bands representing the GFP constructs was quantified. The graph shows the relative intensity of each sample derived from Tm-treated protoplasts with respect to that obtained from untreated protoplasts expressing mGFP5 +  $\alpha$ -amylase (mGFP5 samples) or CLV3-GFP +  $\alpha$ -amylase (CLV3-GFP samples). (D) Protoplasts co-transformed with plasmid encoding CLV3-GFP and increasing amounts (from 0 to 20  $\mu$ g) of plasmid encoding endoplasmic reticulum were incubated in the presence of Tm before pulse-labelling. Immunoprecipitation was with anti-GFP antiserum. The intensity of the bands representing CLV3-GFP was quantified. The graph shows the relative intensity of each sample with respect to that in the first column. (E) As in panel C, but without Tm treatment. In panels C, D and E bars represent standard deviations; values are the mean of four fully independent transformation experiments; one-way ANOVA analysis:  $P < 0.05$  (asterisk) and  $P < 0.01$  (double asterisk).



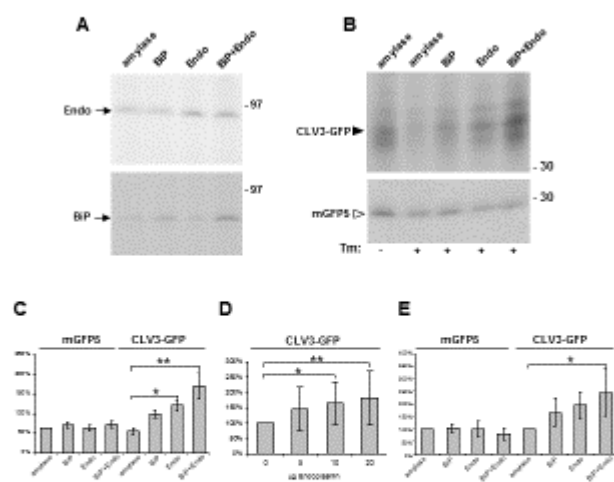


Figure 9

De Marchis F., Colanero S., Klein E.M., Mainieri D., Prota V.M., Bellucci M., Pagliuca G., Zironi E., Gazzotti T., Vitale A., Pompa A., 2018. Erratum to “Expression of CLAVATA3 fusions indicates rapid intracellular processing and a role of ERAD” [Plant Sci. 271 (2018) 67-80]. Plant Science 272, 230–234. DOI: <https://doi.org/10.1016/j.plantsci.2018.04.026>

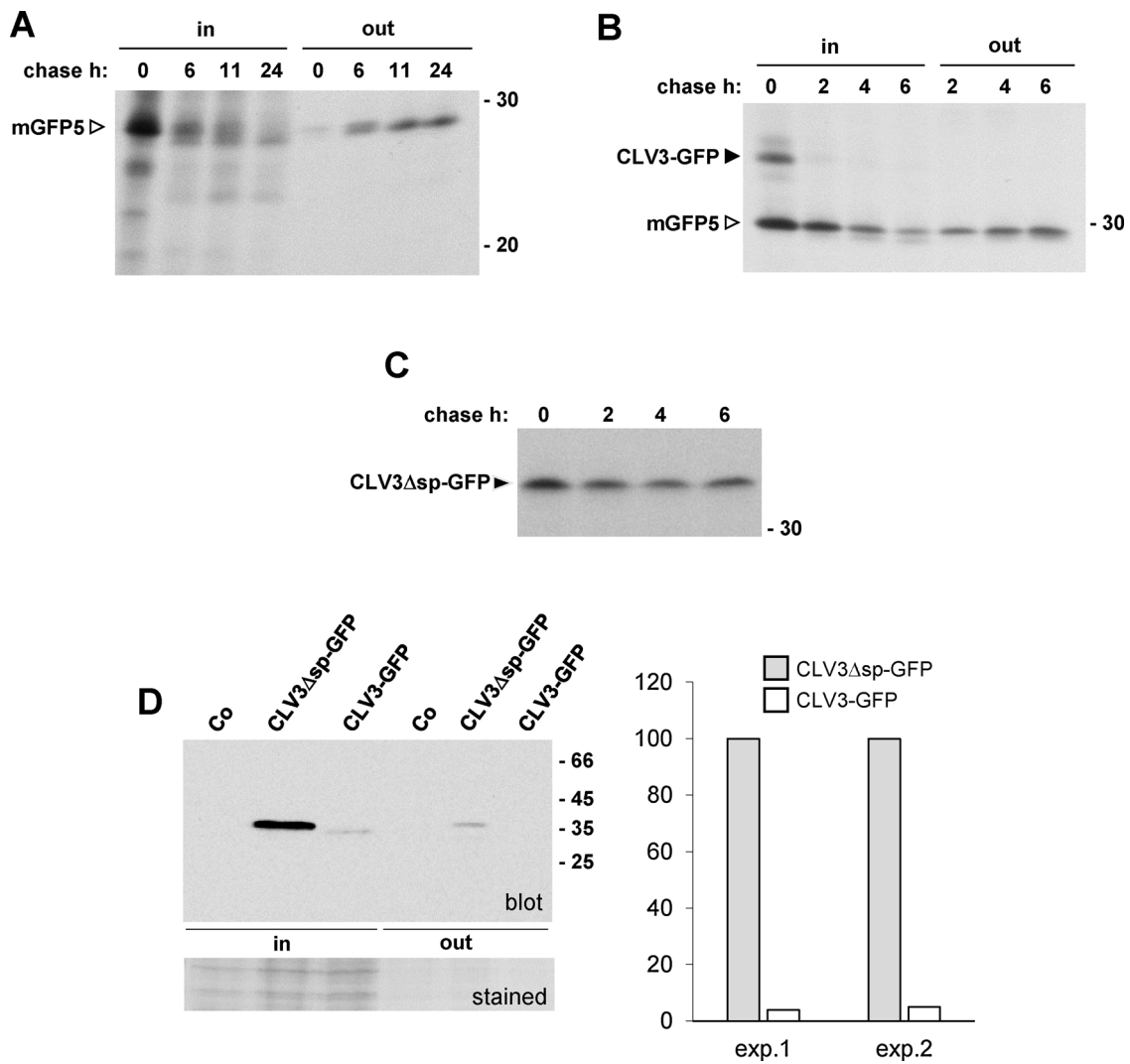


Fig. 2 CLV3-GFP does not perturb protein secretion and is stable when expressed in the cytosol. Tobacco leaf protoplasts were transformed with plasmids encoding the proteins indicated in each panel. A–C: after pulse-labelling for 1 h, chase was performed for the indicated h. Protoplast homogenates or, in panels A and B, homogenates of protoplasts (in) and their incubation medium (out) were immunoselected with anti-GFP serum. After SDS-PAGE, radioactive proteins were detected. (D) Protoplasts were transfected with plasmids encoding the indicated proteins or empty plasmid (Co). After incubation for 24 h, protoplasts (in) or incubation medium (out) were analysed by SDS-PAGE and protein blot with anti-GFP serum. As a loading control, Ponceau S staining is also shown (bottom). Quantitation of CLV3 $\Delta$ sp-GFP or CLV3-GFP in two fully independent protoplast transfections and protein blots is shown at right. In panels A–D, the positions of molecular mass markers (in kD) are shown at right.

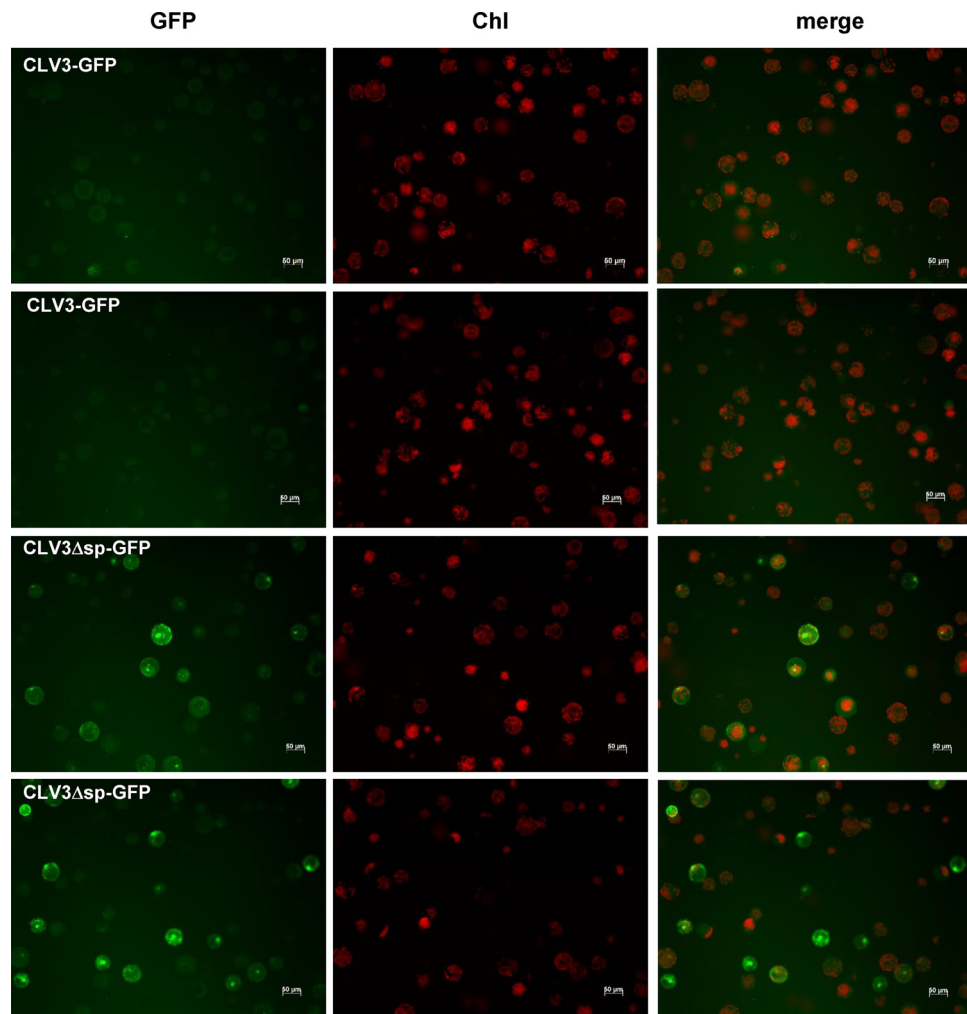


Fig. 3 Fluorescence of CLV3-GFP is almost undetectable in protoplasts. Tobacco leaf protoplasts were transfected with plasmids encoding CLV3-GFP or CLV3 $\Delta$ sp-GFP. After 24 h incubation, fluorescence of GFP or chloroplasts (Chl) was detected by epifluorescence microscopy. Two representative fields are shown for each transformation.

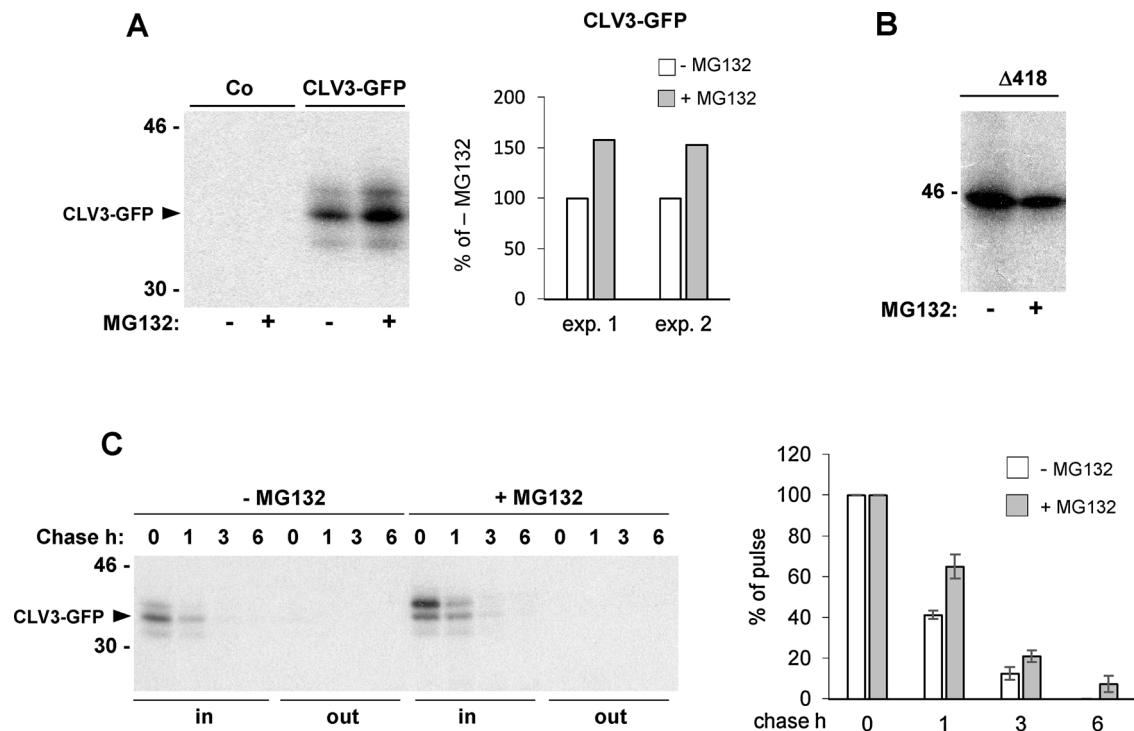


Fig. 6 The proteasome inhibitor MG132 increases CLV3-GFP stability. (A) Protoplasts isolated from leaves of wt tobacco (Co) or transgenic tobacco expressing CLV3-GFP were incubated in the presence or absence of MG132 and pulse-labelled for 1 h. Protoplast homogenates were immunoselected with anti-GFP serum and analysed by SDS-PAGE and fluorography. The graph at right shows, for two fully independent experiments, the relative intensity of radioactive bands, setting the value in the absence of MG132 to 100%. (B) Protoplasts isolated from leaves of transgenic tobacco expressing  $\Delta 418$  phaseolin were incubated in the presence or absence of MG132 and pulse-labelled for 1 h. Protoplast homogenates were immunoselected with anti-phaseolin serum and analysed by SDS-PAGE and fluorography. (C) Pulse-chase of transgenic tobacco protoplast expressing CLV3-GFP. Homogenates (in) and protoplast incubation medium (out) were immunoselected with anti-GFP anti-serum and analysed by SDS-PAGE and fluorography. The graph at right reports quantitation of radioactive bands representing CLV3-GFP in three fully independent experiments, setting the values at 0 h chase to 100%; error bar =  $\pm$  SD. The positions of SDS-PAGE molecular mass markers (in kD) are indicated at left of the gel images.

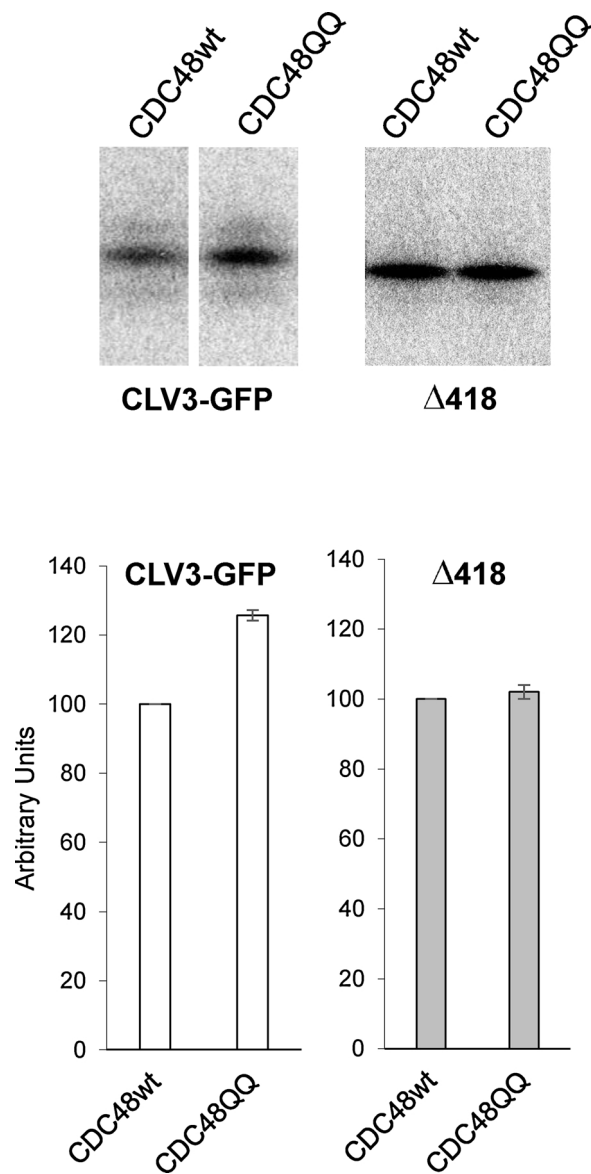


Fig. 8 CDC48QQ increases CLV3-GFP stability. Protoplasts prepared from leaves of transgenic tobacco expressing CLV3-GFP or  $\Delta 418$  phaseolin were co-transfected with plasmids encoding CDC48 wt or CDC48QQ. After pulse-labelling for 1 h with  $[^{35}\text{S}]\text{Met}$  and  $[^{35}\text{S}]\text{Cys}$ , protoplast homogenates were immunoselected with anti-GFP (CLV3-GFP) or anti-phaseolin ( $\Delta 418$ ) serum and analysed by SDS-PAGE and fluorography. For CLV3-GFP, the two images are derived from the same gel and same exposure, after removal of irrelevant lanes. The graphs show the average values of the densitometry analysis from three independent experiments. Error bar =  $\pm$  SD.

The publisher would like to apologise for any inconvenience caused.